Journal of
Breast Cancer

JBC

Original Article

Check for updates

Correspondence to
Hyeong-Gon Moon
Department of Surgery, Seoul National
University College of Medicine, 103 Daehak-ro,
Jongno-gu, Seoul 03080, Korea.
Email: moonhg74@snu.ac.kr

ORCID iDs
Songbin Li 🔟
https://orcid.org/0000-0001-5337-563X
Woochan Lee 🔟
https://orcid.org/0000-0002-1092-7331
Woohang Heo 🔟
https://orcid.org/0000-0002-3296-2015
Hye-Youn Son 🔟
https://orcid.org/0000-0003-4929-0849
Yujeong Her 🔟
https://orcid.org/0000-0002-8478-9525
Jong-Il Kim 🔟
https://orcid.org/0000-0002-7240-3744
Hyeong-Gon Moon 🔟
https://orcid.org/0000-0002-9981-0286

AKR1C2 Promotes Metastasis and Regulates the Molecular Features of Luminal Androgen Receptor Subtype in Triple Negative Breast Cancer Cells

Songbin Li 🔟 [1], Woochan Lee 🔟 [2,3], Woohang Heo 🔟 [4], Hye-Youn Son 🔟 [4], Yujeong Her 🔟 [1], Jong-Il Kim 🔟 [2,3], Hyeong-Gon Moon 🔟 [5,6,7]

[1]Interdisciplinary Graduate Program in Cancer Biology, Seoul National University College of Medicine, Seoul, Korea
[2]Department of Biomedical Sciences, Seoul National University College of Medicine, Seoul, Korea
[3]Genomic Medicine Institute, Medical Research Center, Seoul, Korea
[4]Center for Medical Innovation, Seoul National University Hospital, Seoul, Korea
[5]Cancer Research Institute, Seoul National University, Seoul, Korea
[6]Department of Surgery, Seoul National University Hospital, Seoul, Korea
[7]Department of Surgery, Seoul National University College of Medicine, Seoul, Korea

ABSTRACT

Purpose: Patients with triple-negative breast cancer (TNBC) have an increased risk of distant metastasis compared to those with other subtypes. In this study, we aimed to identify the genes associated with distant metastasis in TNBC and their underlying mechanisms.
Methods: We established patient-derived xenograft (PDX) models using surgically resected breast cancer tissues from 31 patients with TNBC. Among these, 15 patients subsequently developed distant metastases. Candidate metastasis-associated genes were identified using RNA sequencing. *In vitro* wound healing, proliferation, migration, and invasion assays and *in vivo* tumor xenograft and metastasis assays were performed to determine the functional importance of aldo-keto reductase family 1 member C2 (AKR1C2). Additionally, we used the METABRIC dataset to investigate the potential role of AKR1C2 in regulating TNBC subtypes and their downstream signaling activities.
Results: RNA sequencing of primary and PDX tumors showed that genes involved in steroid hormone biosynthesis, including AKR1C2, were significantly upregulated in patients who subsequently developed metastasis. *In vitro* and *in vivo* assays showed that silencing of AKR1C2 resulted in reduced cell proliferation, migration, invasion, tumor growth, and incidence of lung metastasis. AKR1C2 was upregulated in the luminal androgen receptor (LAR) subtype of TNBC in the METABRIC dataset, and AKR1C2 silencing resulted in the downregulation of LAR classifier genes in TNBC cell lines. The androgen receptor (AR) gene was a downstream mediator of AKR1C2-associated phenotypes in TNBC cells. AKR1C2 expression was associated with gene expression pathways that regulate AR expression, including JAK-STAT signaling or interleukin 6 (IL-6). The levels of phospho-signal transducer and activator of transcription and IL-6, along with secreted IL-6, were significantly downregulated in AKR1C2-silenced TNBC cells.
Conclusion: Our data indicate that AKR1C2 is an important regulator of cancer growth and metastasis in TNBC and may be a critical determinant of LAR subtype features.

Keywords: Aldo-Keto Reductase Family 1 Member C2; Neoplasm Metastasis; Receptors, Androgen; Triple Negative Breast Neoplasms

Conflict of Interest

The authors declare that they have no competing interests.

Author Contributions

Conceptualization: Li S, Moon HG; Data curation: Li S, Lee W, Heo W, Son HY, Moon HG; Formal analysis: Li S, Lee W, Heo W, Son HY, Moon HG; Funding acquisition: Kim JI, Moon HG; Investigation: Li S; Methodology: Li S, Lee W, Heo W, Son HY, Her Y; Project administration: Moon HG; Resources: Li S, Lee W, Heo W, Kim JI, Moon HG; Software: Li S, Lee W, Moon HG; Supervision: Son HY, Kim JI, Moon HG; Validation: Li S, Moon HG; Visualization: Li S; Writing - original draft: Li S, Moon HG; Writing - review & editing: Li S, Moon HG.

INTRODUCTION

Breast cancer is the most common malignancy in women worldwide [1]. It is also the most common malignancy in women in Korea, and its incidence has been increasing during the last few decades [2,3]. Although most breast cancers can be effectively treated with current multimodal treatment options, a substantial number of patients eventually develop distant metastasis and die [4].

Triple-negative breast cancer (TNBC) accounts for 10–20% of all breast cancers and is characterized by a lack of estrogen receptor (ER), progesterone receptor (PR), and human epidermal growth factor receptor 2 (HER2) expression. Compared with other subtypes of breast cancer, TNBC has a shorter time to metastasis and recurrence, has fewer treatment options, and is more likely to metastasize to visceral organs such as the lung or liver [5-7]. Therefore, there are ongoing efforts to better understand the molecular mechanisms underlying TNBC.

The patient-derived xenograft (PDX) model is a preclinical research model established by transplanting patient tumor tissue into immunodeficient mice. While some studies have suggested potential limitations of the PDX model in terms of maintaining the biological fidelity of the primary tumors [8,9], many studies have shown that the genetics, gene expression patterns, and histology of PDX tumors are generally stable and can effectively recapitulate the patient's tumor characteristics [10-15]. PDX models can also preserve tumor characteristics, such as cell-cell interactions within the tumor microenvironment, and may provide insights into the mechanisms of drug resistance in cancer [16-18]. Importantly, PDX models of patients with breast cancer have been shown to accurately predict the clinical outcomes of donor patients, suggesting that these models can be effectively used to provide biological insights into the processes of distant metastasis [15,19].

In this study, by performing RNA sequencing using primary tumors and their corresponding PDX tumors, we identified a metastasis-related gene, aldo-keto reductase family 1 member C2 (AKR1C2), in breast cancer. Additionally, our data demonstrate that AKR1C2 regulates androgen receptor (AR) expression and modulates the features of the luminal androgen receptor (LAR) subtype in TNBC.

METHODS

Breast cancer cell lines and small interfering RNA (siRNA) treatment

Breast cancer cell lines were purchased from the Korean Cell Line Bank (Seoul, Korea). MDA-MB-231 and MDA-MB-468 cells were obtained from the American Type Culture Collection (Manassas, VA, USA) and were cultured in Dulbecco's Modified Eagle's medium (Biowest LLC, Riverside, MO, USA) supplemented with 10% fetal bovine serum (FBS; Gibco, Waltham, MA, USA) and 1% penicillin/streptomycin (Gibco). Commercially available AR (gene ID: 367), AKR1C1 (gene ID: 1645), AKR1C3 (gene ID: 8644), and AKR1C4 (gene ID:1109) siRNAs were purchased from Bioneer (Daejeon, Korea). The cells were seeded 1×10^6 cells/well in 6-well plates. After the cells were attached, we diluted Lipofectamine-RNAiMAX Reagent (Invitrogen, Waltham, MA, USA) and siRNA 10 nM (Dharmacon, Lafayette, CO, USA) in Opti-MEM. After incubation for 5 minutes, we treated Lipofectamine and siRNA mixture to attached cells and incubated for 2 days at 37°C. Next, we analyzed the transfected cells.

Cell transfection

The pLKO.1-Puro lentiviral vector was constructed to contain sequences of specific short hairpin RNA (shRNA) targeting human AKR1C2 (**Supplementary Table 1**). Constructs containing pLKO.1-AKR1C2-shRNA were transfected into HEK-293FT cells using Lipofectamine 3000 (Thermo Fisher Scientific, Waltham, MA, USA). After incubation in a CO_2 incubator at 37°C for 48 hours after transfection, the medium containing lentivirus was harvested and used for infecting MDA-MB-231 and MDA-MB-468. Cells with pLKO.1-Puro scramble shRNA (sh-NC) were used as negative controls.

Proliferation assay

Cells were plated in flat-bottom 96-well culture plates (1×10^4 cells per well). The cells were incubated with 0.5 mg/mL thiazolyl blue tetrazolium bromide (MTT; Sigma-Aldrich, St. Louis, MO, USA) for 4 hours at 37°C. The medium was discarded, and 200 μL of dimethyl sulfoxide (Duchefa Biochemie, Haarlem, The Netherlands) was added to each well to dissolve the formazan crystals in the cells. The absorbance was measured at 570 nm using a microplate reader (BioTek Instruments, Winooski, VT, USA).

Cell invasion, migration, and wound healing assay

In the invasion assay, 1 mg/mL Matrigel was added to the insert before seeding the cells, but this was not the case in the migration assay. Medium supplemented with 10% FBS was added to the lower chambers. Cells were incubated for 24 hours, fixed with 4% paraformaldehyde (Biosesang, Seoul, Korea), and stained with 0.1% crystal violet (Sigma-Aldrich). Quantitative evaluation of the migrated and invaded cells was performed using the ImageJ (Java 1.8.0_172) software (NIH, Bethesda, MD, USA).

For the wound healing assay, the cell lines were seeded in 6-well plates. Monolayers were scraped with a pipette tip after 24 hours incubation in a serum-free medium and washed with a serum-free medium to remove floating cells. The cells were photographed every 12 hours at two randomly selected sites per well.

Western blotting, real-time polymerase chain reaction (PCR), and hematoxylin and eosin (H&E) staining

Cell lysates were harvested using radioimmunoprecipitation assay buffer (Thermo Fisher Scientific), protease, and phosphatase inhibitor (Thermo Fisher Scientific), incubated for 10 minutes on ice, and centrifuged at 14,000 rpm for 15 minutes at 4°C. The protein concentration was measured using a bicinchoninic acid assay kit (Thermo Fisher Scientific), separated by sodium dodecyl sulfate-polyacrylamide gel electrophoresis, and transferred to polyvinylidene fluoride (Sigma-Aldrich) membranes. After blocking with 5% bovine serum albumin (Biosesang, Seoul, Korea) solution, membranes were incubated with primary antibody overnight at 4°C. The secondary antibody was diluted (1:10,000) in a 5% skim milk solution. Western blotting bands were detected using an Amersham Imager 680 (GE Healthcare Life Sciences, Chicago, IL, USA). The following antibodies were used: β-actin (#sc-47778; Santa Cruz Biotechnology, Dallas, TX, USA), AKR1C2 (#13035; Cell Signaling Technology, Danvers, MA, USA), AR (#5153; Cell Signaling Technology), signal transducer and activator of transcription 3 (STAT3, #9139; Cell Signaling Technology), phosphorylated STAT3 (pSTAT3, #9138; Cell Signaling Technology), and interleukin 6 (IL-6, #12153; Cell Signaling Technology).

Total RNA was extracted from the cells using TRIzol Reagent (Favorgen, Ping-Tung, Taiwan). The Prime Script 1st strand cDNA Synthesis Kit (Takara, Osaka, Japan) was used for reverse

transcription of RNA, and qPCR assays were performed using Power SYBR Green PCR Master mix (Thermo Fisher Scientific). The reactions were performed using an ABI7500 real-time PCR System (Thermo Fisher Scientific). To compare relative messenger RNA (mRNA) expression levels, gene expression levels were expressed as ratios relative to glyceraldehyde 3-phosphate dehydrogenase. Primer sequences are shown in **Supplementary Table 1**.

Tissues were fixed in 4% para-form aldehyde for 48 hours. After processing, the processed tissues were embedded in paraffin blocks. To identify the histological structure, paraffin blocks were sectioned to a thickness of approximately 4 μm using a microtome. After drying the section slides, paraffin was removed from the sections using xylene, followed by dehydration with ethanol. After dehydration, the nuclei were stained with hematoxylin solution and cytosol with eosin, according to the manufacturer's protocol.

IL-6 enzyme-linked immunosorbent assay (ELISA)

Measurements were performed on the conditioned medium of transfected MDA-MB-231 cells using a Human IL-6 Human ELISA Kit (#EH2IL6; Thermo Fisher Scientific). The conditioned medium was diluted with diluent buffer and added to each well. After incubating for 3 hours at 4°C, each well was washed and incubated for 1 hour at 4°C with human IL-6 conjugate. After washing, substrate solution was added to each well, followed by incubation for 30 minutes. With stop solution addition, each well was read by a microplate reader, followed by calculation of IL-6 concentration with an optical density at 450 nm wavelength.

Established PDX and xenograft murine model

Breast cancer tissues were obtained from surgical specimens obtained during curative or palliative surgery. The acquisition of tissue and clinical and pathologic data from patients with breast cancer for this study was approved by the Institutional Review Board of Seoul National University Hospital (No. H-1707-174-874). Six-week-old female mice were used for the *in vivo* experiments. All experiments involving mouse models were approved by the Institutional Animal Care and Use Committee of the Seoul National University Hospital (No. 19-0096-S1A1, 22-0146-S1A0), and animals were maintained in the facility accredited by AAALAC International (#001169) in accordance with the Guide for the Care and Use of Laboratory Animals 8th edition, NRC (2010).

To establish the PDX model, surgically excised tissue was cut into small pieces of approximately 2 mm and transplanted into NOD/solid IL2Rg mouse mammary fat pads. After the tumor volume reached 1,000 mm³, surgical resection was performed, and the tumor tissue was subjected to transcriptome analysis. To establish a xenograft model, MDA-MB-231 cells stably transfected with sh-NC and shAKR1C2 were injected into the fat pads of 6-week-old athymic female nude mice (1×10^6 cells/mouse). There were five mice each in the control and experimental groups. The length and width of each tumor were measured using calipers, and the volume was calculated using the following equation: V = (length × width²)/2. Tumor volume was measured twice a week until the tumor size reached 1,000 mm³, after which surgical resection was performed. The mice were sacrificed 4 weeks after the operation and lung metastases were observed. MDA-MB-231 cells stably transfected with sh-NC or shAKR1C2 were injected into the tail vein of 6-week-old mice (5×10^5 cells/mouse). There were five mice each in the control and experimental groups. Mice were sacrificed after four weeks, and lung tumor metastasis was observed.

RNA sequencing and bioinformatics

RNA sequencing libraries were prepared using the TruSeq Stranded mRNA Prep kit (Illumina, Inc., San Diego, CA, USA), according to the manufacturer's protocol. Paired-end 101 bp RNA sequencing was performed using a Novaseq 6000 system (Illumina, Inc.). Sequenced RNA reads were aligned to a chimeric reference genome (human hg38 and mouse mm10) using the RSEM-1.3.1. To normalize gene expression levels, we separated raw read counts by the organism and normalized the counts to FPKM using htseq-count. Differentially expressed genes (DEGs) were called using edgeR-3.30.3 for each comparison group.

Statistical analysis

GraphPad Prism ver. 8 (GraphPad Software, San Diego, CA, USA) was to generate graphs and perform statistical tests. Data values are presented as mean ± standard deviation (SD), and Mann-Whitney U tests were used to compare the means between the groups. For the size of tumor volumes, we used two-way analysis of variance (ANOVA) for comparison. Spearman correlation analysis was used to verify the correlation between genes. Survival curves were constructed using the Kaplan–Meier method and compared between TNBC subtypes with the log-rank test. Survival analyses were performed using SPSS 26 (IBM Corp., Armonk, NY, USA).

RESULTS

Gene expression signatures of primary tumors and PDX tumors in patients with TNBC with distant metastases

We established TNBC PDX models using tumor tissues obtained during breast surgery from 31 patients with breast cancer. Subsequently, 15 patients (48.4%) developed distant metastasis during the follow-up period and the remaining 16 patients were disease-free (**Supplementary Table 2**). Since the cells within the tumor microenvironment are replaced by murine stromal cells in PDX tumors, RNA sequencing of PDX tumors can generate gene expression data that are more enriched with epithelial cancer cells by excluding murine sequencing reads [20,21]. Therefore, we hypothesized that incorporating the RNA sequence reads of both PDX tumors and corresponding primary tumors could enrich metastasis-related genes originating from epithelial cancer cells. We obtained 18 corresponding primary tumor tissues from 31 TNBC PDX models and identified 304 genes that were significantly upregulated in both PDX tumors and primary tumors from patients who developed clinical distant metastasis (**Figure 1A**). Interestingly, 304 upregulated genes were enriched with genes involved in steroid hormone biosynthesis (**Figure 1B**, **Supplementary Table 3**). Among the upregulated genes in steroid hormone biosynthesis, AKR1C2 showed the highest level of upregulation (**Figure 1C**, **Supplementary Table 4**).

Among the 31 TNBC PDX models, we were able to catalog the *in vivo* metastasis profiles of 11 PDX models. After serial transplantation, we surgically resected orthotopic tumors at a volume of 1,000 mm³ and maintained the mice to observe the development of metastasis. Six PDX models developed spontaneous metastasis to distant organs, whereas the remaining five did not. The transcriptomic data of the 11 models also indicated that AKR1C2 was significantly upregulated in PDX models that developed *in vivo* metastasis in mice (**Supplementary Figure 1**). These data indicate that AKR1C2 may play an important role in breast cancer metastasis in patients with TNBC.
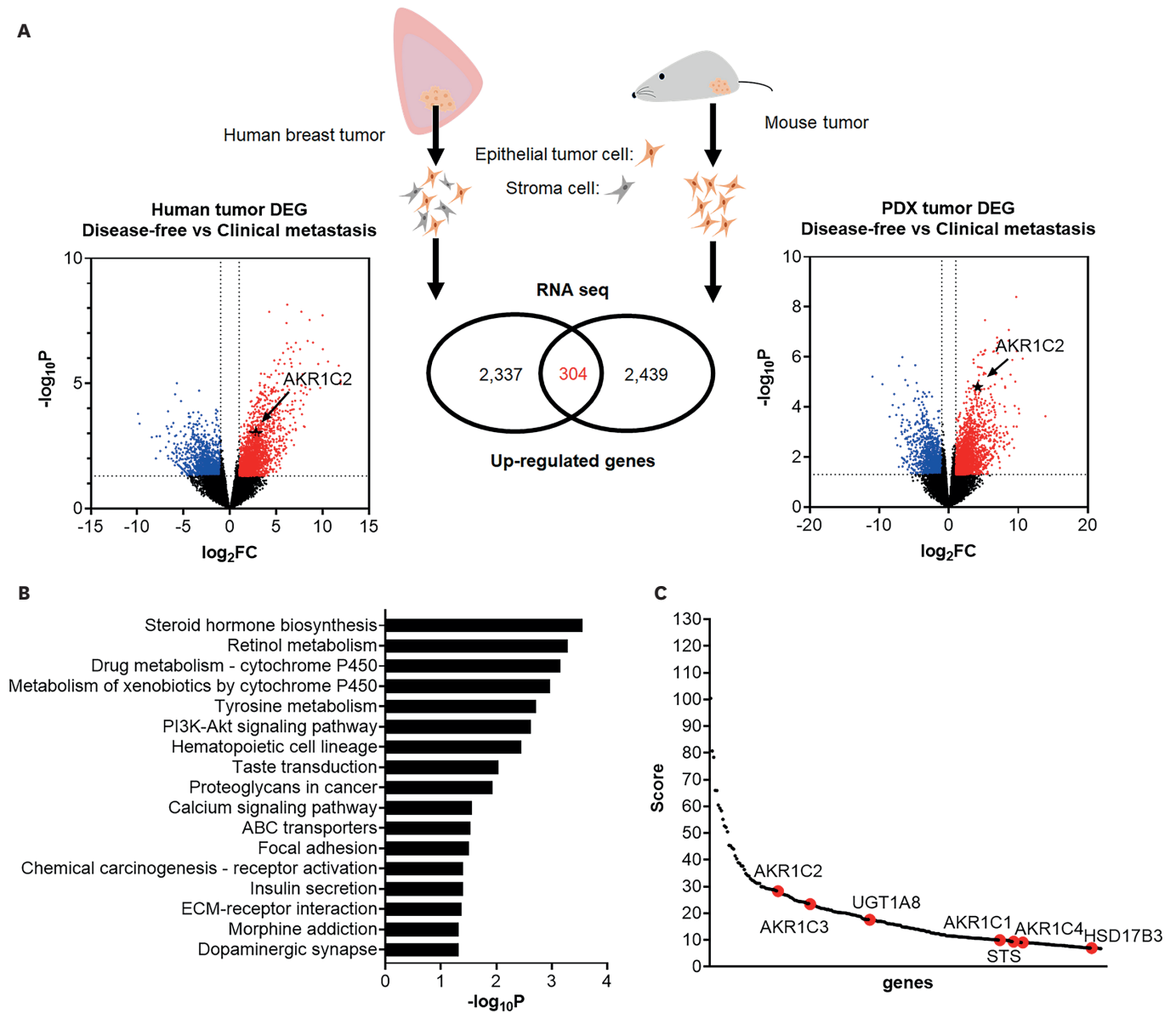
Figure 1. Identification of AKR1C2 as a potential gene regulating breast cancer metastasis.
(A) Schematic illustration of the RNA sequencing experiment. The Venn diagram shows upregulated genes in the tumors that developed distant metastasis, and the volcano plot illustrates the upregulation of AKR1C2. (B) KEGG pathways significantly enriched with the 304 genes that are upregulated in both patient's tumor tissue and PDX tumor tissue. (C) The red dots indicate genes involved in the steroid hormone biosynthetic pathway.
AKR1C2 = aldo-keto reductase family 1 member C2; KEGG = Kyoto Encyclopedia of Genes and Genomes; PDX = patient-derived xenograft.

AKR1C2 promotes *in vitro* growth and migration of TNBC cells

The AKR1C2 gene catalyzes nicotinamide adenine dinucleotide (NADH) and nicotinamide adenine dinucleotide phosphate (NADPH)-dependent conversion from dihydrotestosterone to 3α-diol [22,23]. We examined the expression level of AKR1C2 in a panel of breast cancer cells. Breast cancer cells showed heterogeneous levels of AKR1C2 expression (**Figure 2A**, **Supplementary Figure 2A**). AKR1C2 was significantly upregulated in basal-like (BL) breast cancer cell lines in the CCLE database (**Supplementary Figure 2B**). To determine the functional significance of AKR1C2 in TNBC, we silenced AKR1C2 in MDA-MB-231 cells using shRNA against AKR1C2 (**Figure 2B**, **Supplementary Figure 3A**). Silencing of AKR1C2 significantly reduced the proliferation rate of breast cancer cells (**Figure 2C**). Wound healing
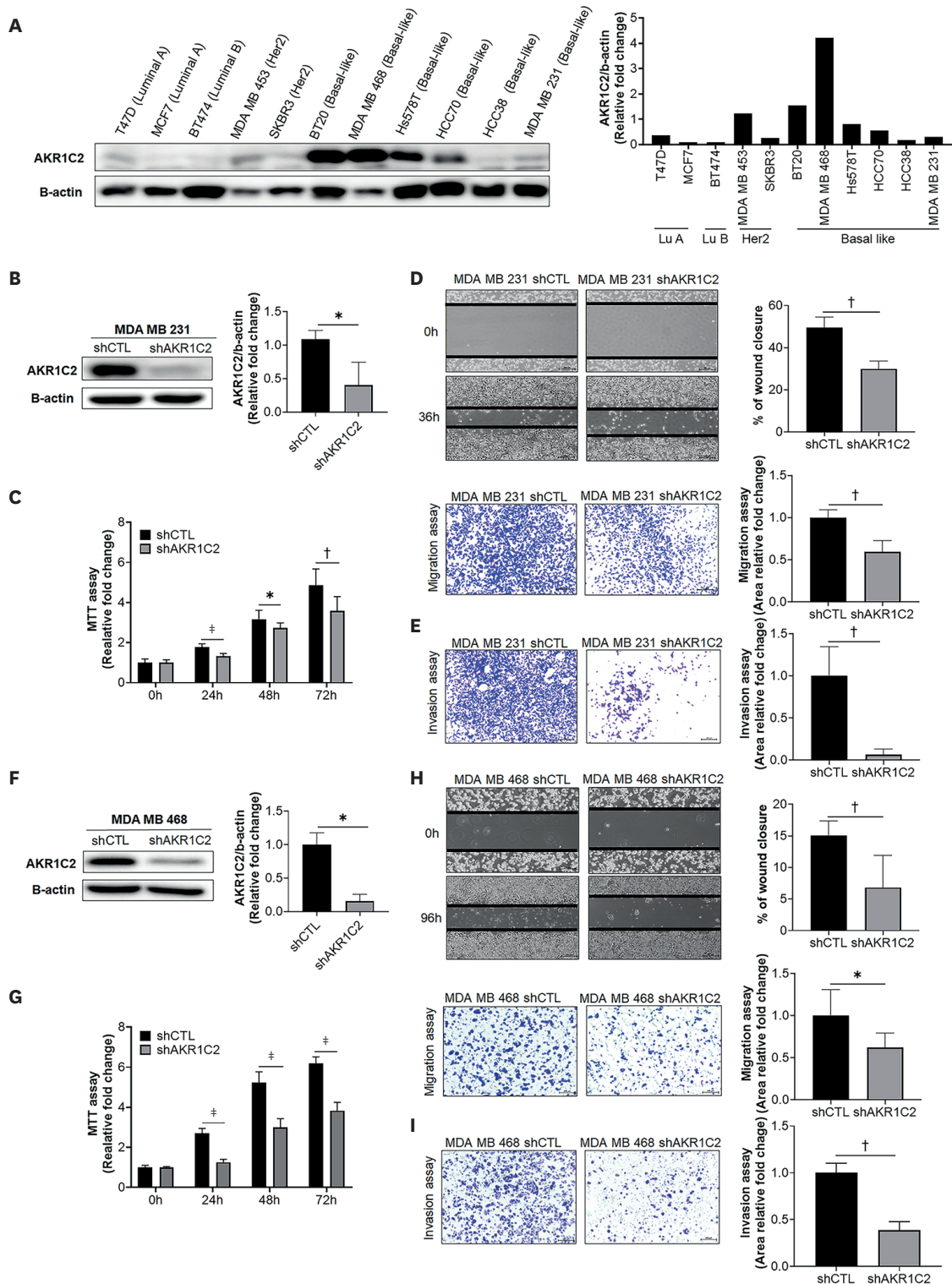
Figure 2. Effect of AKR1C2 on the proliferation, migration, and invasion of TNBC cells.

(A) The AKR1C2 protein expression levels in various breast cancer cell lines. (B) AKR1C2 protein expression levels in shAKR1C2-treated MDA-MB-231 cells. (C) Results of MTT assay using AKR1C2-silenced MDA-MB-231 cells. (D-E). Representative images and quantitative results of wound healing assay, migration assay, and invasion assay using AKR1C2-silenced MDA-MB-231 cells. (F) AKR1C2 protein expression levels in shAKR1C2-treated MDA-MB-468 cells. (G-I) Representative images and quantitative results of MTT assay, wound healing assay, cell migration assay, and cell invasion assay using the AKR1C2-silenced MDA-MB-468 cells. Error bars denote mean ± SD.

AKR1C2 = aldo-keto reductase family 1 member C2; TNBC = triple-negative breast cancer; sh = short hairpin; MTT = thiazolyl blue tetrazolium bromide; SD = standard deviation; CTL = control.

$*p \leq 0.05$, $^{†}p \leq 0.01$, $^{‡}p \leq 0.0001$. p-values were determined by the Mann–Whitney test.

and transwell cell migration assays showed that AKR1C2 silencing resulted in reduced cell migration (**Figure 2D**, **Supplementary Figure 3B**). Additionally, silencing AKR1C2 in MDA-MB-231 cells decreased Matrigel invasion capacity (**Figure 2E**, **Supplementary Figure 3C**). The association between AKR1C2 levels and cancer cell phenotypes *in vitro* was also observed for another TNBC breast cancer cell line, MDA-MB-468 (**Figure 2F-I**, **Supplementary Figure 4**). Finally, we examined whether other genes in the aldo-keto reductase family exert similar effects on TNBC cells by silencing AKR1C1, AKR1C3, and AKR1C4 in TNBC cells. Silencing of these genes resulted in a modest reduction in cell proliferation and invasion, but there was no significant effect on cell migration (**Supplementary Figure 5**). The results of these *in vitro* experiments suggest that AKR1C2 regulates various aspects of breast cancer phenotypes by promoting cell growth and migration in TNBC cells.

AKR1C2 facilitates *in vivo* tumor growth and lung metastasis for MDA-MD-231 cells

Next, we tested whether AKR1C2 expression levels affected the growth and metastasis of breast cancer *in vivo*. We transplanted AKR1C2-silenced and control MDA-MB-231 cells into the fat pads of the nude mice. As shown in **Figure 3A** (**Supplementary Figure 6A**), AKR1C2 silencing significantly reduced the growth of primary tumors. Furthermore, silencing AKR1C2 resulted in a significantly lower number of spontaneous lung metastases (**Figure 3B**, **Supplementary Figure 6B**). To determine the effect of AKR1C2 on the development of lung metastasis, we additionally performed tail vein injection experiments and observed that AKR1C2-silenced breast cancer cells developed a significantly smaller number of lung metastases (**Figure 3C**, **Supplementary Figure 6C**). These data indicate that AKR1C2 regulates primary tumor growth and controls metastasis, which is consistent with the results of the above RNA sequencing data.

AKR1C2 is positively associated with LAR subtypes of TNBC

Steroid hormone biosynthesis regulates the carcinogenesis of TNBC and its molecular classifications [24]. Based on the observation that steroid hormone biosynthesis was the most dysregulated pathway related to the development of distant metastasis and that AKR1C2 plays an important role in cancer cell metastasis *in vivo*, we hypothesized that AKR1C2 can be differentially expressed among the TNBC subtypes. As proposed by Lehmann et al. [25], TNBC can be further classified into six subtypes: two BL (BL1 and BL2), immunomodulatory (IM), mesenchymal (M), mesenchymal stem-like (MSL), and LAR. To test our hypothesis, we obtained gene expression data of 271 TNBC cases from the METABRIC dataset (METABRIC Nature 2012 & Nat Commun 2016) [26] and classified the tumors into different subtypes using the TNBCtype, a web-based subtyping tool for TNBC [27]. The proportions of BL1, BL2, IM, M, MSL, and LAR subtypes were 25.8%, 8.1%, 23.2%, 17.3%, 10.7%, and 14.8%, respectively (**Figure 4A**).

AKR1C2 mRNA levels were significantly different among TNBC subtypes. The LAR subtype showed the highest AKR1C2 levels, whereas the BL1 subtype showed the lowest levels (**Figure 4B**). Next, we examined the correlation between AKR1C2 and TNBC subtype classifier genes used in the study by Lehman et al. [25]. We observed that genes upregulated in the LAR subtype often showed a positive correlation with AKR1C2, but genes for the BL1 subtype often showed a negative correlation, as representative examples such as PIP for the LAR subtype and CENPF for the BL1 subtype are shown in **Figure 4C** (**Supplementary Table 5**). When the correlation coefficients for the subtype-defining genes against AKR1C2 were compared, the LAR subtype genes showed significantly higher correlation coefficients when compared to those of the BL1 subtype (**Figure 4D**). We also measured the mRNA levels of the LAR subtype and BL1 subtype genes in AKR1C2-silenced cells. The expression levels of genes upregulated in the
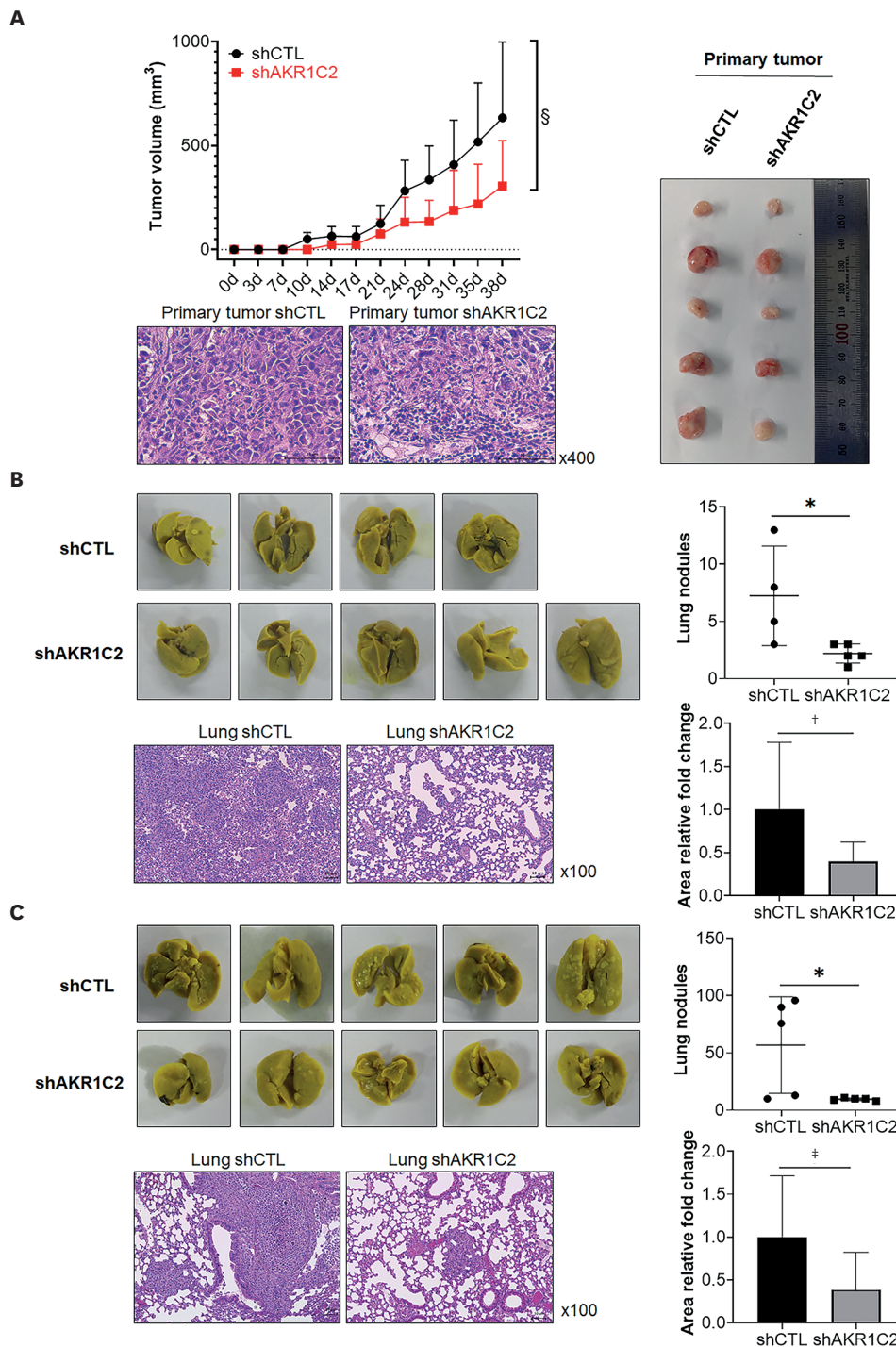
Figure 3. AKR1C2 regulates *in vivo* tumor growth and metastasis in breast cancer cells.

(A) *In vivo* tumor growth for the control and AKR1C2-silenced MDA-MB-231 cells in nude mice. Bottom panels represent representative images of H&E staining of xenograft tumors. (B) Macroscopic and microscopic number of lung nodules in the spontaneous metastasis models. The number and area of metastases were evaluated at one month after the resection of the primary tumors. One of the mice in the control group died during the experiment. (C) Macroscopic and microscopic number of lung nodules in the experimental lung metastasis model of tail-vein injection. The number and area of metastases were evaluated one month after injection. Error bars denote mean ± SD.

AKR1C2 = aldo-keto reductase family 1 member C2; H&E = hematoxylin and eosin; SD = standard deviation; ANOVA = analysis of variance; sh = short hairpin; CTL = control.

*$p \leq 0.05$, †$p \leq 0.001$, ‡$p \leq 0.0001$. *p*-values were determined by ANOVA in **Figure 3A** and by Mann-Whitney test in **Figure 3B and C**.
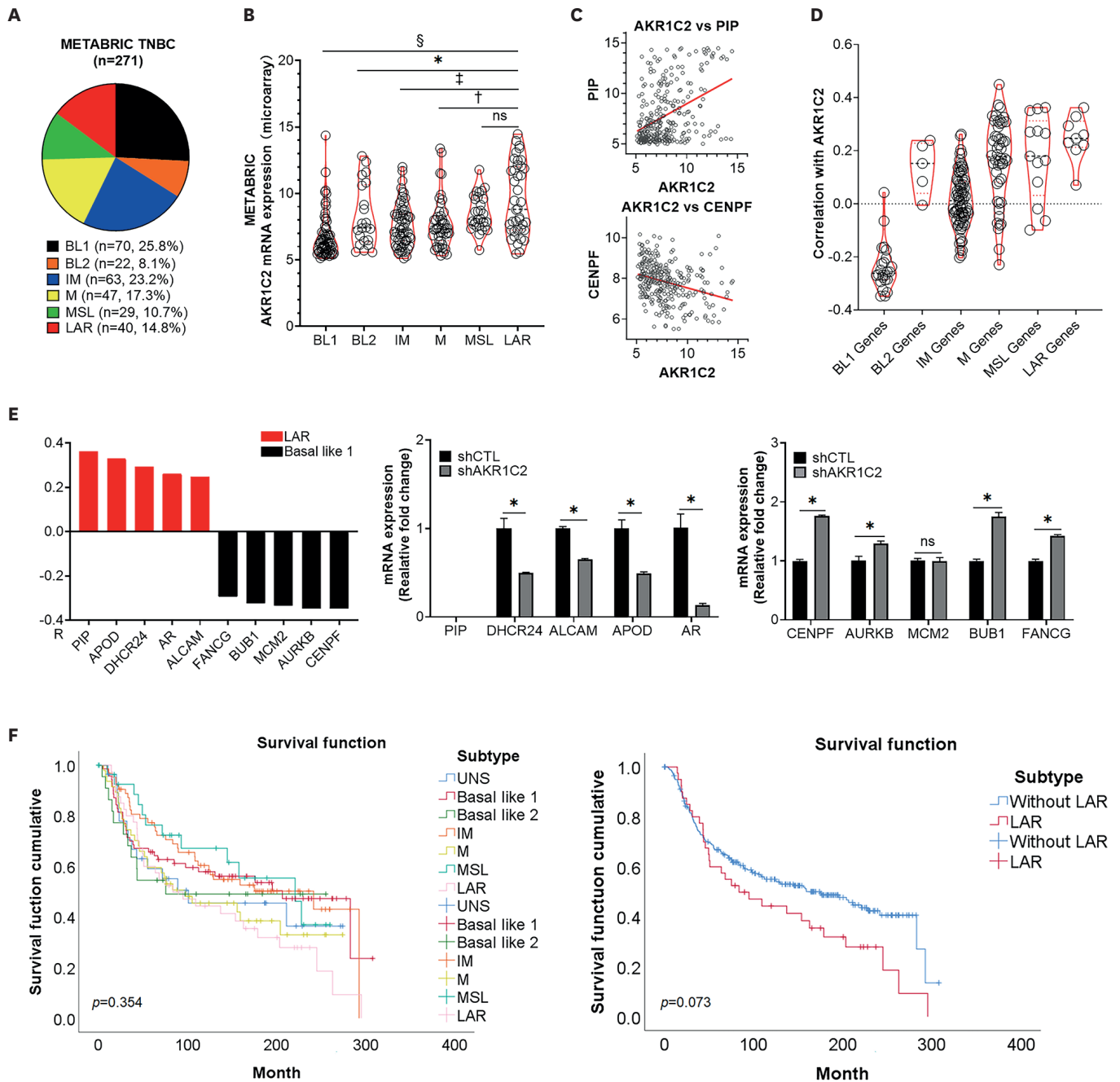
Figure 4. The association between the AKR1C2 and TNBC subtypes.
(A) The prevalence of each TNBC subtypes classified by the TNBC type tool using the METABRIC dataset. (B) AKR1C2 mRNA expression levels in TNBC subtypes. (C) The scatter plot showing the degree of correlation between AKR1C2 and representative genes from LAR (PIP) or BL1 subtype (CENPF). (D) The Spearmen correlation coefficient for the subtype classifier genes and AKR1C2 in TNBC subtypes. (E) The top five LAR subtype-related genes and BL1 subtype-related genes with the highest correlation coefficient R after AKR1C2 correlation analysis and mRNA expression of these genes in AKR1C2-silenced MDA-MB-231. (F) Survival function of TNBC subtypes. The left panel represents survival analysis of TNBC subtypes in the METABRIC dataset. The right panel represents the survival analysis of patients with LAR and other TNBC subtypes. Error bars denote mean ± SD.
AKR1C2 = aldo-keto reductase family 1 member C2; TNBC = triple-negative breast cancer; LAR = luminal androgen receptor; BL = basal-like; mRNA = messenger RNA; SD = standard deviation; IM = immunomodulatory; M = mesenchymal; MSL = mesenchymal stem-like; ns = not significant; UNS = unspecified group.
$*p \leq 0.05$, $†p \leq 0.01$, $‡p \leq 0.001$ $§p \leq 0.0001$. p-values were determined by Spearman correlation, Mann-Whitney, and log-rank test.

LAR subtype, including AR, were significantly downregulated in AKR1C2-silenced breast cancer cells. In contrast, genes that were upregulated in the BL1 subtype were significantly

upregulated in AKR1C2-silenced cells (**Figure 4E**). Consistent with previous reports [28,29], different subtypes of TNBC showed different survival outcomes, with the LAR subtype having the poorest outcomes (**Figure 4F**, **Supplementary Figure 7**). These data indicated that AKR1C2 may play a critical role in determining the subtype characteristics of TNBC cells.

AR, a gene regulated by AKR1C2, controls the proliferation and migration of TNBC cells

AR is a major driver of the molecular features of the LAR subtype in TNBC [23]. We observed decreased AR expression in AKR1C2-silenced breast cancer cells (**Figure 5A**, **Supplementary Figure 8A**). However, AKR1C2 levels were not changed in AR-silenced MDA-MB-231 cells, suggesting an upstream role of AKR1C2 in regulating AR levels (**Figure 5B**, **Supplementary Figure 8B**). Next, we performed *in vitro* assays to determine whether AKR1C2-mediated regulation of AR in breast cancer cells plays a role in the phenotypes observed in AKR1C2-silenced cells. When cells were treated with siAR, MDA-MB-231 cells showed a significant reduction in cell proliferation (**Figure 5C**). Additionally, siAR-treated cells showed decreased transwell migration and Matrigel invasion (**Figure 5D**, **Supplementary Figure 8C**). These data indicate that, at least in part, the phenotypes associated with AKR1C2 silencing may be the result of AKR1C2-mediated AR regulation in breast cancer cells.

Studies [30,31] have shown that AR can be regulated by activated STAT3. Based on the RNA sequencing data comparing the gene expression profiles of AKR1C2-silenced MDA-MB-231 cells to those of control MDA-MB-231 cells, we observed that the genes involved in the JAK-STAT signaling pathway were significantly dysregulated in AKR1C2-silenced cells (**Figure 5E**). Additionally, AKR1C2-silenced cells showed significantly reduced STAT3 phosphorylation (**Figure 5F** and **Supplementary Figure 9A**). Dong et al. [32] suggested a reciprocal interaction between AR and IL-6 which is regulated by STAT3 signaling. Consistently, we observed that AKR1C2-silencing resulted in the downregulation of IL-6 protein (**Figure 5G**, **Supplementary Figure 9B**) and mRNA (**Figure 5H**) levels in breast cancer cells. ELISA results indicated that the amount of secreted IL-6 was also significantly reduced in AKR1C2-silenced cells (**Figure 5I**).

DISCUSSION

In the present study, we attempted to identify the genes associated with breast cancer metastasis using primary tumor tissues and their corresponding PDX tumor tissues. As one can efficiently separate gene expression data originating from epithelial tumor cells and surrounding microenvironment cells [20], integrated analysis of primary tumors and PDX tumors may provide more accurate information on the molecular profiles of epithelial cancer cells. This approach has revealed the importance of JAK2 signaling in regulating paclitaxel resistance in TNBC [18], and Mastri et al. showed that patient-derived models may allow the analysis of epithelial cancer cell pathways independent of the tumor microenvironment [21]. Additionally, the molecular characteristics of the tumor cells are relatively well preserved in the PDX tumor cells [9,15,18,20,21,33], and for some instances, PDX tumors may represent the nature of metastatic clones better than primary tumor tissues [34].

Using this approach, including primary and PDX tumor tissues of 31 patients with breast cancer, we identified AKR1C2 as a potential regulator of distant metastasis in breast cancer. AKR1C2 promoted cancer cell proliferation, migration, and invasion *in vitro*, and AKR1C2 facilitated tumor growth and metastasis *in vivo*. Other members of the AKR1C family have
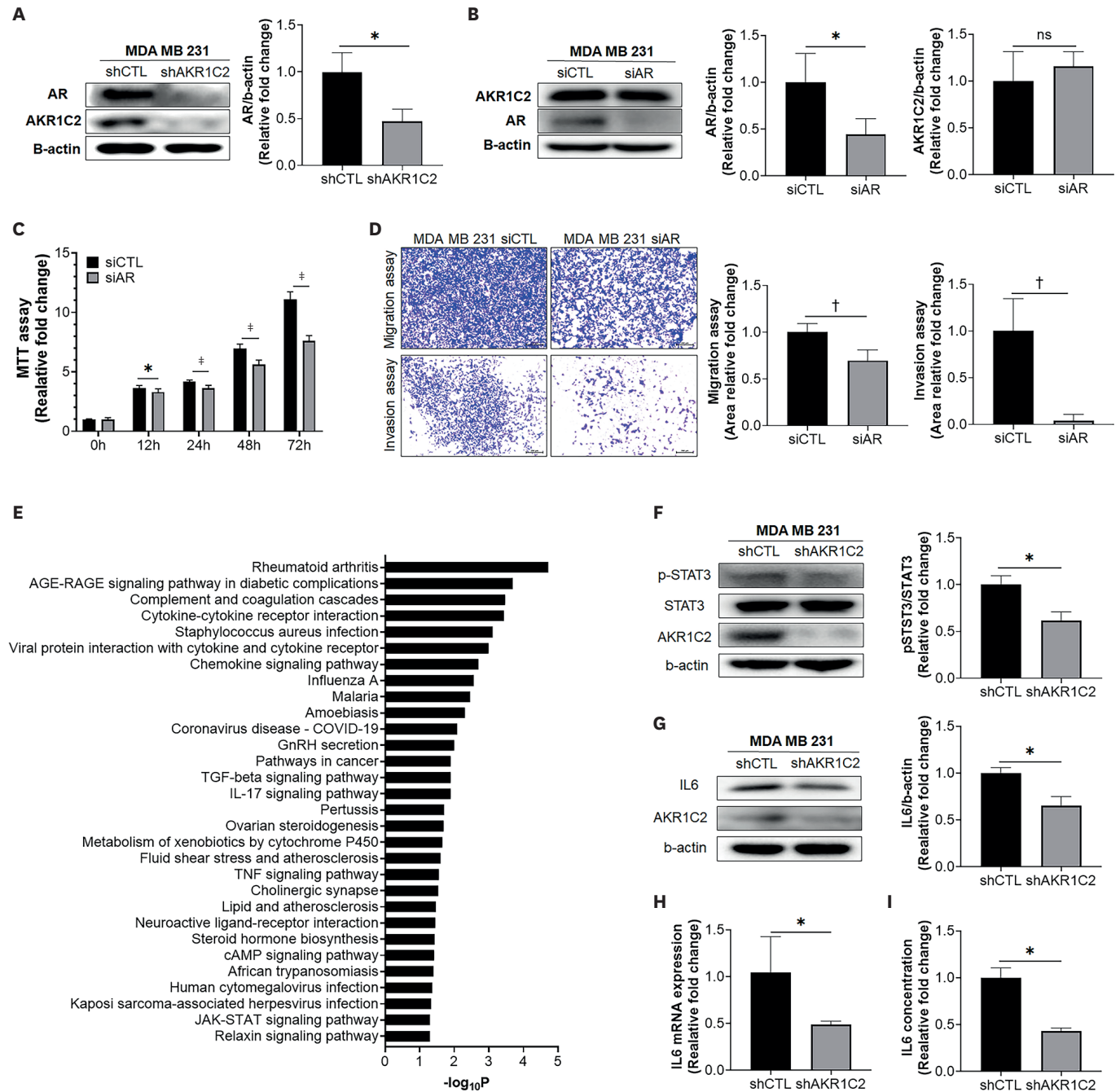
Figure 5. AKR1C2-mediated expression of AR and its effect on breast cancer phenotypes *in vitro*.
(A) AR protein expression levels in AKR1C2-silenced MDA-MB-231 cells. (B) AKR1C2 protein expression levels in AR-silenced MDA-MB-231 cells. (C, D) Effect of AR silencing on MDA-MB-231 breast cancer cell's proliferation (C), migration (D, upper panels), and invasion (D, lower panels). (E) KEGG pathway analysis of downregulated genes in xenograft tumor tissues. (F) pSTAT3 and STAT3 protein expression levels in AKR1C2-silenced MDA-MB-231 cells. (G) IL-6 protein expression levels in AKR1C2-silenced MDA MB 231 cells. (H) IL-6 mRNA expression levels in AKR1C2-silenced MDA-MB-231 cells. (I) IL-6 concentration in AKR1C2-silenced MDA-MB-231-conditioned medium. Error bars denote mean ± SD.
AKR1C2 = aldo-keto reductase family 1 member C2; AR = androgen receptor; pSTAT = phosphorylated signal transducer and activator of transcription 3; STAT3 = signal transducer and activator of transcription 3; IL-6 = interleukin 6; mRNA = messenger RNA; SD = standard deviation; ns = not significant; si = small interfering; CTL = control.
$^{*}p \leq 0.05$, $^{†}p \leq 0.01$, $^{‡}p \leq 0.0001$. *p*-values were determined by Mann-Whitney test.

a corresponding effect on breast cancer progression, but not as significant as AKR1C2. Our data indicate that AKR1C2, a steroid hormone biosynthesis gene that catalyzes NADH and

NADPH-dependent conversion of dihydrotestosterone to 3α-diol, may play an important role in the development of distant metastasis in TNBC.

However, the role of AKR1C2 in various solid tumor types remains controversial. It has been reported that in malignant tumors, such as prostate cancer and esophageal cancer, AKR1C2 can promote tumor growth and metastasis by regulating epithelial mesenchymal transition or affecting the phosphoinositide 3-kinase (PI3K)/Akt signaling pathway [35-37]. Although we observed similar pro-tumorigenic effects of AKR1C2 in TNBC cells in the present study, AKR1C2 had no effect on PI3K/Akt signaling in TNBC cells. In this study, AKR1C2 was shown to regulate AR expression. Studies have shown that AKR1C2 can directly interact with STAT3 and phosphorylate STAT3 [38]. pSTAT3 can modulate AR activation in the absence of hormones [30,31,39]. In the present study, AKR1C2 affected the JAK-STAT pathway and pSTAT3. This may be the mechanism that affects TNBC metastasis. On the other hand, some studies have suggested that AKR1C2 may exert inhibitory effects on tumors, as AKR1C2 expression is associated with improved prognosis in thyroid cancer [40] and AKR1C2 overexpression results in slower tumor growth in prostate cancer [41,42]. Further research on the role of AKR1C2 in human solid tumors is required to clarify its importance in different tumor types.

Additionally, our data suggested that AKR1C2 may influence the subtype determination of TNBC cells. Although efforts have been made to clarify the origins of the different intrinsic subtypes of breast cancer [43,44], the molecular mechanisms underlying the classification of the TNBC subtype are largely unknown. Since Lehman et al. [25] proposed that TNBC can be further classified into different subtypes, studies have repeatedly shown the presence of heterogeneity and its clinical implications [29,45]. In the present study, AKR1C2 was highly upregulated in the LAR subtype, whereas it was significantly downregulated in the BL1 subtype. Furthermore, AKR1C2 silencing resulted in the downregulation of genes expressed in the LAR subtype, including AR. These observations indicate that AKR1C2 expression levels may determine the subtypes of TNBC cells, as PDGF signaling is suggested to regulate the conversion of basal breast cancer to luminal cancer [46]. The potential association between AKR1C2 and LAR subtypes and their therapeutic implications should be tested in future studies.

Our study has several limitations. First, although our data suggest that AKR1C2 regulates AR expression, the mechanism by which it affects AR has not yet been elucidated. Second, we could not address the functional importance of AKR1C2 in non-basal subtypes because we focused our assays on TNBC cell lines. Finally, we were unable to determine the prognostic importance of AKR1C2 in an independent cohort of patients with breast cancer.

In conclusion, our data indicated that AKR1C2 is an important regulator of cancer growth and metastasis in TNBC cells. AKR1C2 regulates the expression of AR in breast cancer cells and is associated with the LAR subtype of TNBC. Future research on the potential therapeutic use of targeting AKR1C2 in patients with TNBC is warranted.

SUPPLEMENTARY MATERIALS

Supplementary Table 1
Information on used primer sequences

Click here to view

Supplementary Table 2

Patients' age, DFS, and metastatic site

Click here to view

Supplementary Table 3

Pathway analysis of 304 upregulated genes

Click here to view

Supplementary Table 4

AKR1C2 showed the highest upregulation of steroid hormone biosynthesis

Click here to view

Supplementary Table 5

Correlation analysis between TNBC subtype-related genes and AKR1C2

Click here to view

Supplementary Figure 1

To investigate whether the AKR1C family is differentially expressed in PDX models.

Click here to view

Supplementary Figure 2

Expression of AKR1C2 in breast cancer cell lines.

Click here to view

Supplementary Figure 3

Effect of AKR1C2 on the viability, migration ability, and invasion ability of MDA-MB-231.

Click here to view

Supplementary Figure 4

Effect of AKR1C2 on the viability, migration ability, and invasion ability of MDA-MB-468.

Click here to view

Supplementary Figure 5

Effect of AKR1C family-related genes in breast cancer.

Click here to view

Supplementary Figure 6

Morphology and lung metastasis of tumor cells in xenograft models established by AKR1C2-silenced MDA-MB-231.

Click here to view

Supplementary Figure 7

Prognosis of TNBC subtypes in the METABRIC dataset.

Click here to view

Supplementary Figure 8

Effect of AR on the viability, migration ability, and invasion ability of MDA-MB-231.

Click here to view

Supplementary Figure 9

Protein expression levels of pSTAT3 and IL-6 in AKR1C2-silenced MDA-MB-231.

Click here to view

REFERENCES

1. Sung H, Ferlay J, Siegel RL, Laversanne M, Soerjomataram I, Jemal A, et al. Global cancer statistics 2020: GLOBOCAN estimates of incidence and mortality worldwide for 36 cancers in 185 countries. CA Cancer J Clin 2021;71:209-49.
   PUBMED | CROSSREF

2. Jung KW, Won YJ, Hong S, Kong HJ, Im JS, Seo HG. Prediction of cancer incidence and mortality in Korea, 2021. Cancer Res Treat 2021;53:316-22.
   PUBMED | CROSSREF

3. Kang SY, Lee SB, Kim YS, Kim Z, Kim HY, Kim HJ, et al. Breast cancer statistics in Korea, 2018. J Breast Cancer 2021;24:123-37.
   PUBMED | CROSSREF

4. Lee SB, Kim HK, Choi Y, Ju YW, Lee HB, Han W, et al. Dynamic and subtype-specific interactions between tumour burden and prognosis in breast cancer. Sci Rep 2020;10:15445.
   PUBMED | CROSSREF

5. Kumar P, Aggarwal R. An overview of triple-negative breast cancer. Arch Gynecol Obstet 2016;293:247-69.
   PUBMED | CROSSREF

6. Foulkes WD, Smith IE, Reis-Filho JS. Triple-negative breast cancer. N Engl J Med 2010;363:1938-48.
   PUBMED | CROSSREF

7. Dent R, Trudeau M, Pritchard KI, Hanna WM, Kahn HK, Sawka CA, et al. Triple-negative breast cancer: clinical features and patterns of recurrence. Clin Cancer Res 2007;13:4429-34.
   PUBMED | CROSSREF

8. Shi J, Li Y, Jia R, Fan X. The fidelity of cancer cells in PDX models: characteristics, mechanism and clinical significance. Int J Cancer 2020;146:2078-88.
   PUBMED | CROSSREF

9. Eirew P, Steif A, Khattra J, Ha G, Yap D, Farahani H, et al. Dynamics of genomic clones in breast cancer patient xenografts at single-cell resolution. Nature 2015;518:422-6.
   PUBMED | CROSSREF

10. Okada S, Vaeteewoottacharn K, Kariya R. Application of highly immunocompromised mice for the establishment of patient-derived xenograft (PDX) models. Cells 2019;8:889.
    PUBMED | CROSSREF

11. Aparicio S, Hidalgo M, Kung AL. Examining the utility of patient-derived xenograft mouse models. Nat Rev Cancer 2015;15:311-6.
    PUBMED | CROSSREF

12. Byrne AT, Alférez DG, Amant F, Annibali D, Arribas J, Biankin AV, et al. Interrogating open issues in cancer precision medicine with patient-derived xenografts. Nat Rev Cancer 2017;17:254-68.
    PUBMED | CROSSREF

13. Blomme A, Van Simaeys G, Doumont G, Costanza B, Bellier J, Otaka Y, et al. Murine stroma adopts a human-like metabolic phenotype in the PDX model of colorectal cancer and liver metastases. Oncogene 2018;37:1237-50.
    PUBMED | CROSSREF

14. Yoshida GJ. Applications of patient-derived tumor xenograft models and tumor organoids. J Hematol Oncol 2020;13:4.
    PUBMED | **CROSSREF**

15. Moon HG, Oh K, Lee J, Lee M, Kim JY, Yoo TK, et al. Prognostic and functional importance of the engraftment-associated genes in the patient-derived xenograft models of triple-negative breast cancers. Breast Cancer Res Treat 2015;154:13-22.
    PUBMED | **CROSSREF**

16. Jung J, Seol HS, Chang S. The generation and application of patient-derived xenograft model for cancer research. Cancer Res Treat 2018;50:1-10.
    PUBMED | **CROSSREF**

17. Kerbel RS. Human tumor xenografts as predictive preclinical models for anticancer drug activity in humans: better than commonly perceived-but they can be improved. Cancer Biol Ther 2003;2:S134-9.
    PUBMED | **CROSSREF**

18. Han J, Yun J, Quan M, Kang W, Jung JG, Heo W, et al. JAK2 regulates paclitaxel resistance in triple negative breast cancers. J Mol Med (Berl) 2021;99:1783-95.
    PUBMED | **CROSSREF**

19. DeRose YS, Wang G, Lin YC, Bernard PS, Buys SS, Ebbert MT, et al. Tumor grafts derived from women with breast cancer authentically reflect tumor pathology, growth, metastasis and disease outcomes. Nat Med 2011;17:1514-20.
    PUBMED | **CROSSREF**

20. Cho SY, Chae J, Na D, Kang W, Lee A, Min S, et al. Unstable genome and transcriptome dynamics during tumor metastasis contribute to therapeutic heterogeneity in colorectal cancers. Clin Cancer Res 2019;25:2821-34.
    PUBMED | **CROSSREF**

21. Mastri M, Ramakrishnan S, Shah SD, Karasik E, Gillard BM, Moser MT, et al. Patient derived models of bladder cancer enrich the signal of the tumor cell transcriptome facilitating the analysis of the tumor cell compartment. Am J Clin Exp Urol 2021;9:416-34.
    PUBMED

22. Tchernof A, Mansour MF, Pelletier M, Boulet MM, Nadeau M, Luu-The V. Updated survey of the steroid-converting enzymes in human adipose tissues. J Steroid Biochem Mol Biol 2015;147:56-69.
    PUBMED | **CROSSREF**

23. Penning TM, Byrns MC. Steroid hormone transforming aldo-keto reductases and cancer. Ann N Y Acad Sci 2009;1155:33-42.
    PUBMED | **CROSSREF**

24. Christenson JL, Trepel JB, Ali HY, Lee S, Eisner JR, Baskin-Bey ES, et al. Harnessing a different dependency: how to identify and target androgen receptor-positive versus quadruple-negative breast cancer. Horm Cancer 2018;9:82-94.
    PUBMED | **CROSSREF**

25. Lehmann BD, Bauer JA, Chen X, Sanders ME, Chakravarthy AB, Shyr Y, et al. Identification of human triple-negative breast cancer subtypes and preclinical models for selection of targeted therapies. J Clin Invest 2011;121:2750-67.
    PUBMED | **CROSSREF**

26. Curtis C, Shah SP, Chin SF, Turashvili G, Rueda OM, Dunning MJ, et al. The genomic and transcriptomic architecture of 2,000 breast tumours reveals novel subgroups. Nature 2012;486:346-52.
    PUBMED | **CROSSREF**

27. Chen X, Li J, Gray WH, Lehmann BD, Bauer JA, Shyr Y, et al. TNBCtype: a subtyping tool for triple-negative breast cancer. Cancer Inform 2012;11:147-56.
    PUBMED | **CROSSREF**

28. Lehmann BD, Jovanović B, Chen X, Estrada MV, Johnson KN, Shyr Y, et al. Refinement of triple-negative breast cancer molecular subtypes: implications for neoadjuvant chemotherapy selection. PLoS One 2016;11:e0157368.
    PUBMED | **CROSSREF**

29. Lehmann BD, Colaprico A, Silva TC, Chen J, An H, Ban Y, et al. Multi-omics analysis identifies therapeutic vulnerabilities in triple-negative breast cancer subtypes. Nat Commun 2021;12:6276.
    PUBMED | **CROSSREF**

30. Hobisch A, Eder IE, Putz T, Horninger W, Bartsch G, Klocker H, et al. Interleukin-6 regulates prostate-specific protein expression in prostate carcinoma cells by activation of the androgen receptor. Cancer Res 1998;58:4640-5.
    PUBMED

31. Lee SO, Lou W, Hou M, de Miguel F, Gerber L, Gao AC. Interleukin-6 promotes androgen-independent growth in LNCaP human prostate cancer cells. Clin Cancer Res 2003;9:370-6.
    PUBMED

32. Dong H, Xu J, Li W, Gan J, Lin W, Ke J, et al. Reciprocal androgen receptor/interleukin-6 crosstalk drives oesophageal carcinoma progression and contributes to patient prognosis. J Pathol 2017;241:448-62.
    PUBMED | CROSSREF

33. Kopetz S, Lemos R, Powis G. The promise of patient-derived xenografts: the best laid plans of mice and men. Clin Cancer Res 2012;18:5160-2.
    PUBMED | CROSSREF

34. Ding L, Ellis MJ, Li S, Larson DE, Chen K, Wallis JW, et al. Genome remodelling in a basal-like breast cancer metastasis and xenograft. Nature 2010;464:999-1005.
    PUBMED | CROSSREF

35. Zhang ZF, Huang TJ, Zhang XK, Xie YJ, Lin ST, Luo FF, et al. AKR1C2 acts as a targetable oncogene in esophageal squamous cell carcinoma via activating PI3K/AKT signaling pathway. J Cell Mol Med 2020;24:9999-10012.
    PUBMED | CROSSREF

36. Li C, Wu X, Zhang W, Li J, Liu H, Hao M, et al. High-content functional screening of AEG-1 and AKR1C2 for the promotion of metastasis in liver cancer. J Biomol Screen 2016;21:101-7.
    PUBMED | CROSSREF

37. Li C, Tian ZN, Cai JP, Chen KX, Zhang B, Feng MY, et al. Panax ginseng polysaccharide induces apoptosis by targeting Twist/AKR1C2/NF-1 pathway in human gastric cancer. Carbohydr Polym 2014;102:103-9.
    PUBMED | CROSSREF

38. Zhu H, Chang LL, Yan FJ, Hu Y, Zeng CM, Zhou TY, et al. AKR1C1 activates STAT3 to promote the metastasis of non-small cell lung cancer. Theranostics 2018;8:676-92.
    PUBMED | CROSSREF

39. Xu Y, Qi W, Wang X, Zhang Y, Han L, Shi J, et al. Signal transducer and activator of transcription 3 cooperates with androgen receptor/cell cycle-related kinase signalling pathway in the progression of hepatitis B virus infection and gender differences. J Viral Hepat 2022;29:569-78.
    PUBMED | CROSSREF

40. Jin YX, Zhou XF, Chen YY, Jin WX, Wang YH, Ye DR, et al. Up-regulated AKR1C2 is correlated with favorable prognosis in thyroid carcinoma. J Cancer 2019;10:3543-52.
    PUBMED | CROSSREF

41. Rizner TL, Lin HK, Penning TM. Role of human type 3 3alpha-hydroxysteroid dehydrogenase (AKR1C2) in androgen metabolism of prostate cancer cells. Chem Biol Interact 2003;143-144:401-9.
    PUBMED | CROSSREF

42. Bremmer F, Jarry H, Unterkircher V, Kaulfuss S, Burfeind P, Radzun HJ, et al. Testosterone metabolites inhibit proliferation of castration- and therapy-resistant prostate cancer. Oncotarget 2018;9:16951-61.
    PUBMED | CROSSREF

43. Sims AH, Howell A, Howell SJ, Clarke RB. Origins of breast cancer subtypes and therapeutic implications. Nat Clin Pract Oncol 2007;4:516-25.
    PUBMED | CROSSREF

44. Skibinski A, Kuperwasser C. The origin of breast tumor heterogeneity. Oncogene 2015;34:5309-16.
    PUBMED | CROSSREF

45. Yin L, Duan JJ, Bian XW, Yu SC. Triple-negative breast cancer molecular subtyping and treatment progress. Breast Cancer Res 2020;22:61.
    PUBMED | CROSSREF

46. Roswall P, Bocci M, Bartoschek M, Li H, Kristiansen G, Jansson S, et al. Microenvironmental control of breast cancer subtype elicited through paracrine platelet-derived growth factor-CC signaling. Nat Med 2018;24:463-73.
    PUBMED | CROSSREF